



## HYDROGEN DETECTION WITH A GAS SENSOR ARRAY – PROCESSING AND RECOGNITION OF DYNAMIC RESPONSES USING NEURAL NETWORKS

Patryk Gwiżdż, Andrzej Brudnik, Katarzyna Zakrzewska

AGH University of Science and Technology, Faculty of Computer Science, Electronics and Telecommunications, Department of Electronics, Mickiewicza Av. 30, 30-059 Krakow, Poland (✉ gwizdz@agh.edu.pl, +48 12 617 2594)

### Abstract

An array consisting of four commercial gas sensors with target specifications for hydrocarbons, ammonia, alcohol, explosive gases has been constructed and tested. The sensors in the array operate in the dynamic mode upon the temperature modulation from 350°C to 500°C. Changes in the sensor operating temperature lead to distinct resistance responses affected by the gas type, its concentration and the humidity level. The measurements are performed upon various hydrogen (17-3000 ppm), methane (167-3000 ppm) and propane (167-3000 ppm) concentrations at relative humidity levels of 0-75%RH. The measured dynamic response signals are further processed with the Discrete Fourier Transform. Absolute values of the dc component and the first five harmonics of each sensor are analysed by a feed-forward back-propagation neural network. The ultimate aim of this research is to achieve a reliable hydrogen detection despite an interference of the humidity and residual gases.

Keywords: gas sensor, sensor array, temperature modulation, dynamic response, feature extraction, neural networks.

© 2015 Polish Academy of Sciences. All rights reserved

### 1. Introduction

Gas sensors based on metal oxides are well known for their high sensitivity to reducing and oxidizing gases. However, the lack of a selectivity and – especially – an interference of the humidity are their largest drawbacks [1, 2]. Therefore, the discrimination between several chemicals - the presence of which is detected by metal oxide sensors - is difficult to perform, unless an array of sensors is used. On the other hand, the cross-sensitivity of these sensors is exploited in electronic noses [3] and sensor arrays [4–6]. Typically, the performance of metal oxide gas sensors can be improved by their construction. This may involve using nanostructured materials which offer an increased sensitivity and selectivity [9–11]. However, the overall performance of metal oxide gas sensors can be enhanced without a modification of the sensor construction. One of the techniques used is a modulation of the sensor temperature [5–7]. It is well known that the gas sensitivity characteristics of metal oxide sensors, as well as the kinetics of adsorption reactions [7] at the sensor surface, are affected by the operating temperature. Therefore, a modulation of the operating temperature induces a dynamic response which is characteristic for a gas mixture composition and a humidity level [5, 6]. The pattern recognition plays an important role in the data processing of metal oxide gas detection systems and electronic noses [8].

Gas sensors usually operate in the air at the environmental humidity. It is generally accepted that under these operating conditions various uncontrolled species such as oxygen, water and carbon dioxide are present. Essentially, the sensor response is strongly influenced by the humidity [12, 13], affecting the performance of metal oxide gas sensors. As a result of a temperature modulation and different sensing properties at various temperatures, changing

the sensor resistance depends on the applied temperature profile and the overall gas atmosphere composition. In order to improve the sensing performance the sensor dynamic responses are processed and examined by means of digital signal processing techniques. It was reported that it was possible to discriminate gases by processing the sensor response with the Fast Fourier Transform (FFT) [18–21] coupled with neural networks [22–24]. Artificial neural networks are dynamic and self-adapting systems that resemble the process of human learning and are capable of machine learning and the pattern recognition. Different types of neural networks were used for data processing in electronic nose systems and metal oxide gas sensor arrays [14–17, 22–24].

In this work the performance of an array of metal oxide sensors operating upon the induced sinusoidal temperature profile is studied. The feature extraction from the dynamic response is performed with the Discrete Fourier Transform (DFT) and the pattern recognition is achieved by a feed-forward back-propagation neural network. The ultimate aim is to demonstrate that exploiting the cross-sensitivity and the temperature induced dynamic response combined with the feature extraction and the pattern recognition enables a reliable hydrogen detection in spite of an interference of the humidity and residual gases. Moreover, the presented method enables the evaluation of the humidity level.

## 2. Experimental details

An array consisting of four metal oxide gas sensors with different target gas specifications from UST (Umweltsensortechnik) was designed, constructed and tested [6]. Each sensor has an incorporated platinum heater which allows to measure and control its temperature. The sensors used in the array and their specifications are listed in Table 1.

Table 1. The specification of the sensors used in the array.

Sensor symbol	Description
GGs 1000	a universal sensor for detecting leaks of combustible gases, such as hydrogen, methane and carbon monoxide
GGs 3000	a sensor for hydrocarbons and hydrogen, optimized for hydrocarbons
GGs 4000	a selective sensor for ammonia, with a low cross-sensitivity to CH <sub>4</sub> , CO and H <sub>2</sub>
GGs 8000	a sensor for detecting C <sub>2</sub> H <sub>5</sub> OH, with a low sensitivity to CH <sub>4</sub> , CO and H <sub>2</sub>

The array is connected to a measuring-control system; its block diagram is presented in Fig. 1. The system built by the authors consists of a four-channel gas flow controller with four MKS Instruments 1179A mass flow gauges, a humidity and temperature logger, a temperature controller, a resistance measuring unit and a PC computer for the data acquisition.

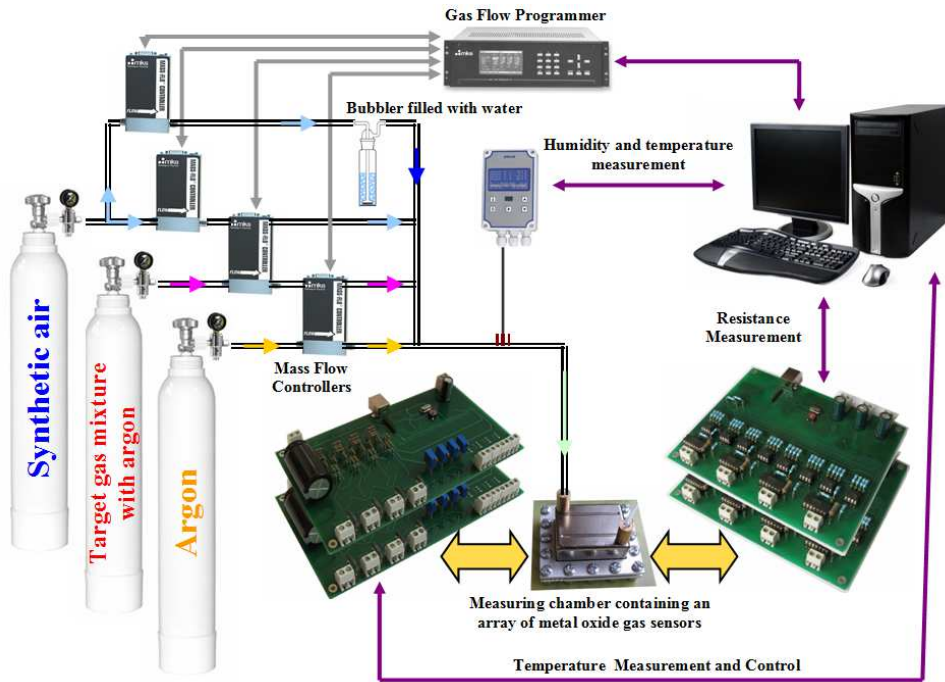


Fig. 1. A block diagram of the experimental setup.

The sensors in the array operate in the dynamic mode upon the temperature modulation. The temperature of each sensor is deduced from the resistance of its platinum heater. Since the applied voltage and the current flowing through each sensor are measured, the heater resistance can be determined. The sensor operating temperature is derived from the equation (1) which describes the relationship [25] between the heater temperature  $T_H$  and its resistance  $R_H$ :

$$T_H = -\left(\frac{A}{2B} + \sqrt{\frac{A^2}{4B^2} - \frac{R_{H0} - R_H}{B \cdot R_{H0}}}\right), \quad (1)$$

where:  $R_{H0}$  – the heater resistance at 0 °C,  $A = 3.9083 \times 10^{-3} \text{ °C}^{-1}$ ,  $B = -5.775 \times 10^{-7} \text{ °C}^{-2}$ . Based on measurement results of the sensor operating temperature a controlled sinusoidal temperature profile is imposed independently for each sensor. The temperature of each sensor is modulated from 350°C to 500°C in the period of 3 minutes. During the measurements the gas sensing atmosphere is created by mixing the synthetic air with the target gas ( $\text{H}_2$ ,  $\text{CH}_4$ ,  $\text{C}_3\text{H}_8$ ) and argon. This is done in order to obtain the same oxygen concentration in the gas atmosphere. The flow of the synthetic air is kept constant (40 sccm) while the additional total gas flow of 20 sccm is produced by adjusting the gas flows of pure Ar and the target gas + Ar mixture. The target gas mixtures used during the experiments include 0.1%  $\text{H}_2$  in Ar, 1%  $\text{H}_2$  in Ar, 1%  $\text{CH}_4$  in Ar and 1%  $\text{C}_3\text{H}_8$  in Ar. Various humidity levels of 0-75%RH are set by mixing, at certain proportions, the dry synthetic air with the synthetic air flowing through a bubbler filled with water and thus saturated to 100%RH. The relative humidity is measured with a HIH-4602 sensor from Honeywell. The dynamic responses are studied as a function of the hydrogen (17–3000 ppm), methane (167–3000 ppm) and propane (167–3000 ppm) concentration at various humidity levels (0–75%RH). A detailed description of the gas sensing properties of the array operating at a constant temperature can be found in [6].

### 3. Results and discussion

In the experiment all sensors in the array operate upon an induced temperature profile in a so-called dynamic operation mode. In this mode of operation a controlled sinusoidal change of the operating temperature of each sensor is imposed. This leads to periodic changes in the electrical resistance of the sensors, as shown in Fig. 2. The periodic dynamic resistance changes induced by the temperature profile are described in [5, 6].

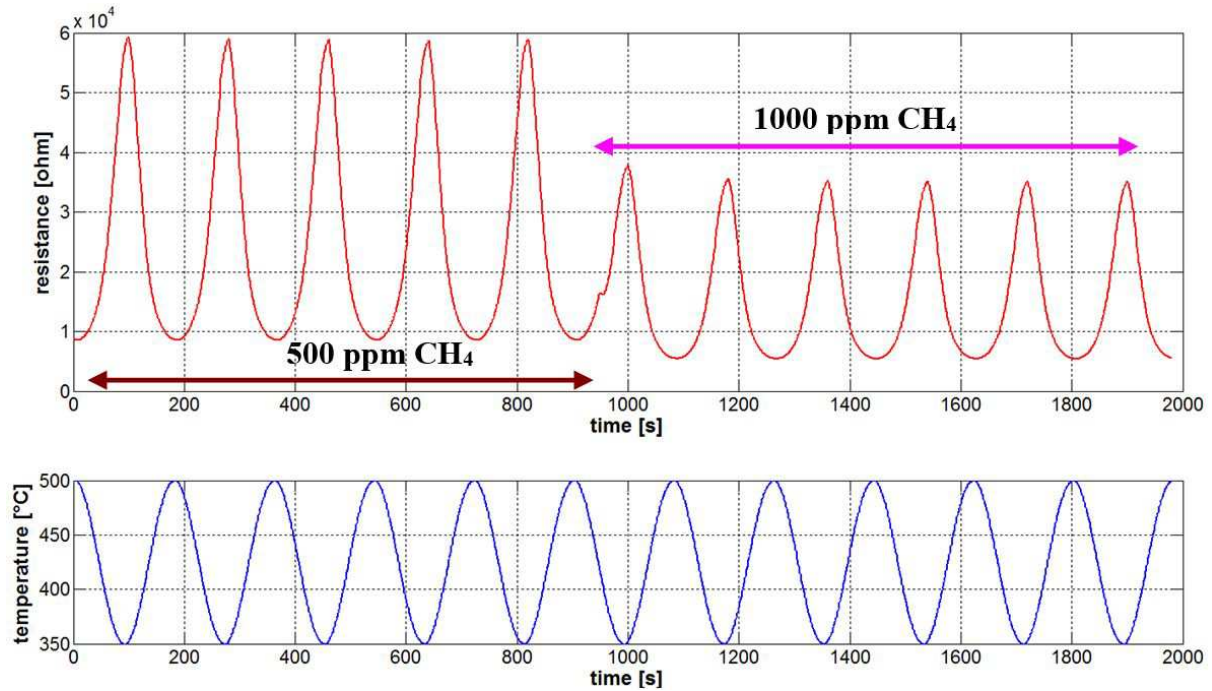


Fig. 2. The dynamic response of an GGS 3000 sensor to 500 and 1000 ppm of CH<sub>4</sub> at 0 %RH upon the sinusoidal temperature modulation (350 - 500°C).

The dynamic resistance changes of metal oxide gas sensors depend on the target gas concentration, as presented in Fig. 2 for methane, and also on its type. These resistance changes over one temperature modulation cycle are further processed.

#### 3.1. Signal processing

The duration of one temperature modulation cycle is set to 3 minutes and the resistance sampling frequency is 1 Hz. So, the resistance change over one temperature modulation period  $\mathbf{r}$  consists of  $N = 180$  samples:

$$\mathbf{r} = [r_1 \ r_2 \ \dots \ r_N]_{1 \times N} \quad (2)$$

These resistance changes over one temperature modulation cycle for different hydrogen, methane and propane concentrations at humidity levels of 0 and 75%RH are presented in Fig. 3.

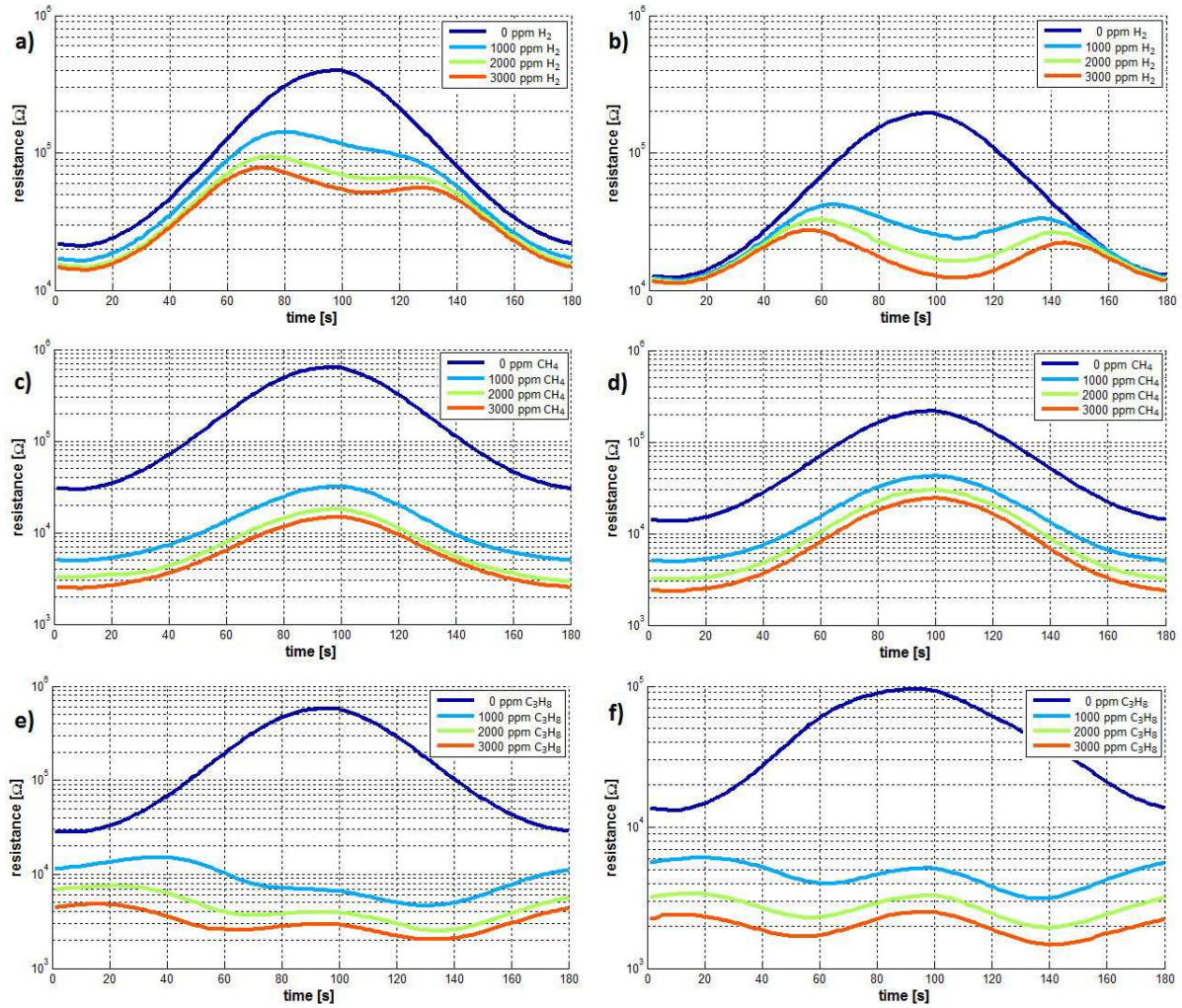


Fig. 3. The dynamic responses of an GGS 3000 sensor over one temperature modulation cycle (350 - 500°C) to different concentrations of: a) hydrogen 0%RH, b) hydrogen 75%RH, c) methane 0%RH, d) methane 75%RH, e) propane 0%RH, f) propane 75%RH.

As one can observe in Fig. 3, the response amplitude depends on the gas type and its concentration, as well as on the relative humidity level. Furthermore, changes in the dynamic resistance response curve can be noticed. In order to compare these response curve shape changes, the sensor responses are pre-processed according to the following formula:

$$s_{Ri} = \frac{r_i - \min(\mathbf{r})}{\max(\mathbf{r}) - \min(\mathbf{r})} \quad (i = 1, 2, \dots, N), \quad (3)$$

where:  $r_i$  is the  $i$ -th element of the resistance change  $\mathbf{r}$  over one temperature modulation cycle,  $s_{Ri}$  is the  $i$ -th element of the pre-processed normalized response  $\mathbf{s}_R$ ,  $\min(\mathbf{r})$  and  $\max(\mathbf{r})$  are the minimum and the maximum values of  $\mathbf{r}$ . The result of the performed pre-processing is the pre-processed normalized sensor response  $\mathbf{s}_R$ :

$$\mathbf{s}_R = [s_{R1} \quad s_{R2} \quad \dots \quad s_{RN}]_{1 \times N}. \quad (4)$$

In a consequence, the value of each sample  $s_{Ri}$  in the pre-processed normalized response  $\mathbf{s}_R$  is contained within the interval  $[0, 1]$ . Examples of normalized responses of an GGS 3000 sensor over one temperature modulation cycle for different concentrations of hydrogen, methane and propane at the humidity levels of 0 and 75%RH are presented in Fig. 4.

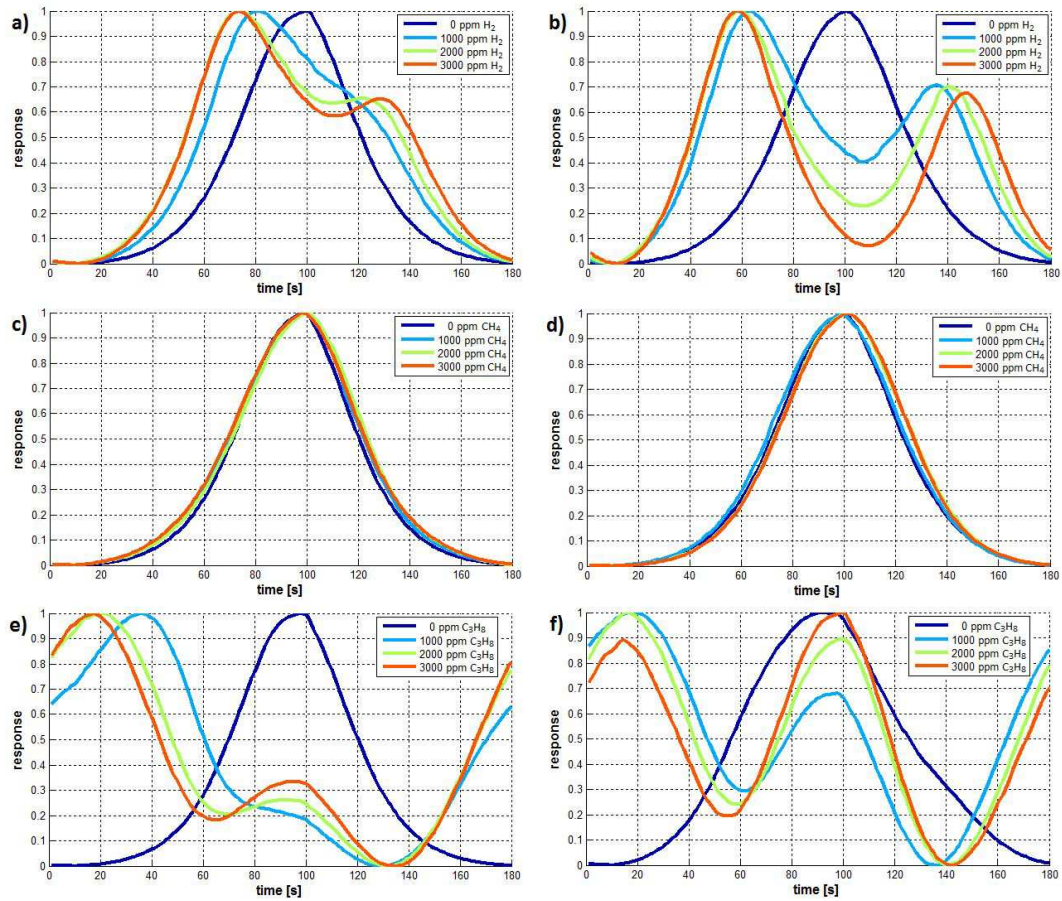


Fig. 4. The dynamic normalized responses of an GGS 3000 sensor over one temperature modulation cycle (350 - 500°C) to different concentrations of: a) hydrogen 0%RH, b) hydrogen 75%RH, c) methane 0%RH, d) methane 75%RH, e) propane 0%RH, f) propane 75%RH.

As one can observe in Fig. 4, for hydrogen and propane the shape of the normalized response curve depends on both the target gas concentration and the humidity level. Furthermore, for methane no changes in the normalized response curve shape are observed for an GGS 3000.

In order to perform a feature extraction from the normalized response  $s_R$  of each sensor the Discrete Fourier Transform (DFT) has been derived according to the formula:

$$S_{mk} = \sum_{i=1}^N s_{Ri} \cdot e^{-j2\pi \frac{k}{N} i} \quad (k = 1, 2, \dots, N), \quad (5)$$

where:  $S_{mk}$  is the k-th element of the discrete spectrum  $S_m$  of the m-th sensor.

In order to analyse the influence of subsequent harmonics on the response spectrum it is advantageous to use the values of  $H_{mk}$  being the k-th harmonic content of the m-th sensor in the response spectrum, defined as:

$$H_{mk} = \frac{S_{mk}}{\sum_{i=1}^{\frac{N}{2}} |S_{mi}|} \cdot 100\% \quad (k = 1, 2, \dots, \frac{N}{2}). \quad (6)$$

Using the values as a criterion we were allowed to conclude that only the first five harmonics and the dc component carry most of the information on the processed signal of each sensor.

Therefore, only the absolute values of those five coefficients from DFT and the dc component of each sensor response constitute an input  $s_{IN}$  for the neural network, which is given by:

$$s_{IN} = [s_{10} \quad s_{11} \quad s_{12} \quad s_{13} \quad s_{14} \quad s_{15} \quad \dots \quad s_{mk}], \quad (7)$$

where:  $s_{mk}$  is the  $k$ -th element of the discrete spectrum of the  $m$ -th sensor. The scheme of the described signal processing method applied to a four-element sensor array is summarized in Fig. 5.

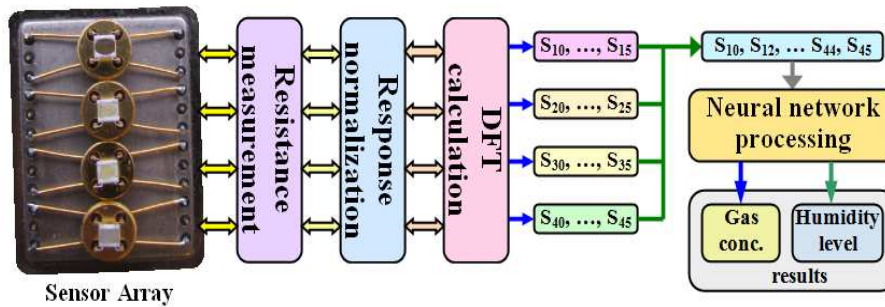


Fig. 5. A diagram of the signal processing method used in the experiment.

### 3.2. Gas detection and recognition

In order to facilitate a selective and reliable hydrogen detection in spite of interfering factors like: methane, propane and a humidity, as well as the humidity level, a feed-forward back-propagation neural network has been applied and the Levenberg-Marquardt learning algorithm has been used. A feed-forward back-propagation neural network consists of an input layer, one or more hidden layers and an output layer. In a feed-forward neural network, neurons are connected forward and there are no connections backward. In other words, each layer contains connections only to the next layer. The term back-propagation corresponds to the training type of a neural network. The back-propagation algorithm is a form of supervised training for multilayer neural networks. When this type of learning is applied, the network must be provided with sample inputs and anticipated outputs. Using the anticipated outputs, the back-propagation training calculates the error (the anticipated outputs are compared with the actual outputs for a given input) and adjusts weights of various layers backwards from the output layer to the input layer.

In our research the performance of neural networks with various numbers of hidden layers was studied using the Matlab software. The measurements of the sensor response to hydrogen, methane and propane (using 1% mixtures of target gas with argon) were conducted for the following concentrations: 0, 167, 500, 1000, 1167, 1500, 2000, 2333, 2500 and 3000 ppm. Moreover, using the mixture of 0.1% hydrogen in argon the sensor responses were recorded at the concentrations of 0, 17, 50, 100, 117, 150, 200, 233, 250, 300 ppm  $H_2$ . The responses at each concentration were measured at the relative humidity levels of 0, 25, 50, 75%RH. In total, the sensor responses have been measured at 160 different gas atmosphere compositions. The learning set consisted of 2240 input signals while the testing and the validation sets consisted of 480 signals each recorded at various hydrogen, methane and propane concentrations and humidity levels. Gas concentration and humidity level predictions of feed-forward back-propagation neural networks with 1 to 40 hidden layers were tested. At the beginning the influence of the number of analysed harmonics on the hydrogen and humidity prediction was studied. The average prediction error of all neural networks with 1 to 40 hidden layers vs. the number of analysed harmonics is presented in Fig. 6.

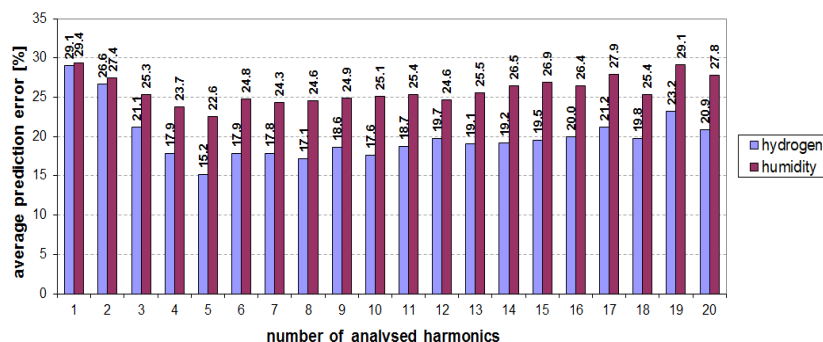


Fig. 6. An average gas concentration and humidity prediction error vs. the number of harmonics used as an input for the neural networks with 1 to 40 hidden layers.

As presented in Fig. 6, the average hydrogen prediction error has the smallest value of 15.2% when five harmonics of each sensor response are analysed. However, only slightly bigger error of 17.9% is obtained when four and six harmonics are analysed. In terms of the humidity prediction also the smallest average error (22.6%) is obtained when five harmonics are analysed. As one can observe, a certain number of harmonics has to be analysed. It is clear that if the analysed number of harmonics is either too small or too big, the neural networks tend to give bigger prediction errors of the hydrogen concentration and the humidity level. The relation between the number of analysed harmonics and the neural networks giving the best performance is illustrated in Fig. 7. As the best performance it is assumed that the neural network gives the lowest hydrogen prediction error but not necessarily the lowest humidity prediction error.

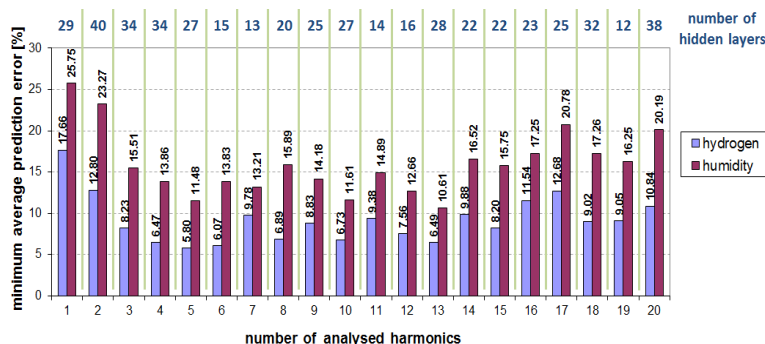


Fig. 7. An average gas concentration and humidity prediction error of the networks with 1 to 40 hidden layers giving the best performance vs. the number of analysed harmonics.

As presented in Fig. 7, the lowest average hydrogen concentration prediction error of 5.80% is achieved when five harmonics are analysed. However, only a slightly higher error is achieved when four or six harmonics are analysed. We assume that the best neural network should give the lowest humidity and gas concentration error.

Finally, we can conclude that the best performance is achieved for a neural network with 27 hidden layers analysing the absolute value of five harmonics and the dc component of the dynamic response spectrum of each sensor in the array. This neural network can predict the hydrogen concentration and humidity level with an average error of 5.80% and 11.48% respectively.

At last, the influence of the learning and testing sets on the neural network performance has been studied. During the neural network training the measured data set is divided into three subsets (training, validation and testing). The training subset is used during the learning stage for computing the gradient and updating the network weights and biases. The validation subset is used to calculate the validation error during the training process. The testing subset

is not used during the training process, but in comparing the studied neural networks. The size of the testing subset is the same as the validation subset. The measured data are divided randomly into those three subsets. The initial set consisted of 3200 measured data at various gas atmosphere compositions. Initially, at each target gas concentration and humidity level 20 responses were measured. Next, the initial set was systematically reduced in such a way that at each tested gas atmosphere composition the number of measured responses was reduced by two. Therefore, the smallest data set consisted of only two responses measured for each gas atmosphere composition. The results concerning the average prediction error for neural networks with 1 to 40 hidden layers versus the learning and testing sets are presented in Fig. 8.

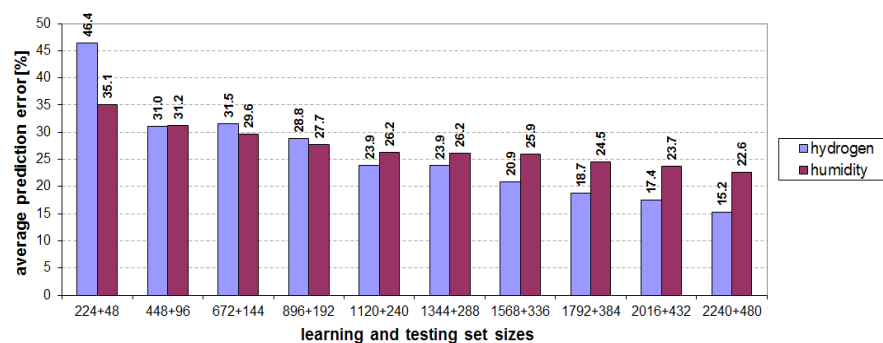


Fig. 8. An average gas concentration and humidity prediction error.

As one can see in Fig. 8, the neural network performance depends on the size of the learning set used during the network training stage.

#### 4. Conclusions

The obtained results let us to conclude that the array of metal oxide gas sensors operating upon an induced sinusoidal temperature profile combined with a feature extraction and the pattern recognition enables a reliable determination of the hydrogen concentration with an average error below 5.8% despite an interference of the humidity and interfering gases, such as methane and propane. Moreover, the results of our work indicate that not only the gas detection can be achieved but also – simultaneously - the determination of the relative humidity level with an average error of 11.5%.

#### 5. Acknowledgment

Patryk Gwiżdż acknowledges the support of Polish Ministry of Science and Education under the AGH-University of Science and Education grant for PhD students (15.11.230.142) for 2014 and benefits from the financial support from "Doctus - Małopolski Fundusz stypendialny dla doktorantów". This work has been also financed by Polish National Center for Science, NCN, grant decision DEC-2011/03/B/ST7/01840.

#### References

- [1] Barsan, N., Koziej, D., Weimar, U., (2007). Metal oxide-based gas sensor research: How to? *Sensor. Actuat. B-Chem.*, (121), 18–35.
- [2] Wang, C., Yin, L., Zhang, L., Xiang, D., Gao, R., (2010). Metal Oxide Gas Sensors: Sensitivity and influencing factors. *Sensors*, (10), 2088–2106.

- [3] Sobański, T., Szczurek, A., Nitsch, K., Licznerski, B.W., Radwan, W., (2006). Electronic nose applied to automotive fuel qualification. *Sensor. Actuat. B-Chem.*, (116), 207–212.
- [4] Szczurek, A., Maciejewska, M., (2004). Recognition of benzene, toluene and xylene using TGS array integrated with linear and non-linear classifier. *Talanta*, (64), 609–617.
- [5] Gwiżdż, P., Brudnik, A., Zakrzewska, K., (2012). Temperature modulated response of gas sensors array - humidity interference. *Proc. Eng.*, (47), 1045–1048.
- [6] Gwiżdż, P., Brudnik, A., Zakrzewska, K., (2012). Temperature-modulated gas sensor array. *Microelectron. Mater. Technol.*, Wydawnictwo Uczelniane Politechniki Koszalińskiej, (1), 196–206.
- [7] An, W., Yang, C., (2012). Review on temperature modulation technology of gas sensors. *App. Mech. Mater.*, (143-144), 567–571.
- [8] Shi, Z. B., Yu, T., Zhao, Q., Li, Y., Lan, Y. B., (2008). Comparison of Algorithms for an Electronic Nose in Identifying Liquors. *J. Bio. Eng.*, (5), 253–257.
- [9] Lyson-Sypien, B., Czapla, A., Lubecka, M., Gwiżdż, P., Schneider, K., Zakrzewska, K., Michalow, K., Graule, T., Reszka, A., Rekas, M., Lacz, A., Radecka, M., (2012). Nanopowders of chromium doped TiO<sub>2</sub> for gas sensors. *Sensor. Actuat. B-Chem.*, (175), 163–172.
- [10] Jasiński, P., Suzuki, T., Anderson, H. U., (2003). Nanocrystalline undoped ceria oxygen sensor. *Sensor. Actuat. B-Chem.*, (95), 73–77.
- [11] Calavia, R., Mozalev, A., Vazquez, R., Gracia, I., Cané, C., Ionescu, R., Llobet, E., (2010). Fabrication of WO<sub>3</sub> nanodot-based microsensors highly sensitive to hydrogen. *Sensor. Actuat. B-Chem.*, (149), 352–361.
- [12] Koziej, D., Barsan, N., Weimar, U., Szuber, J., Shimanoe, K., Yamazoe, N., (2005). Water–oxygen interplay on tin dioxide surface: Implication on gas sensing. *Chem. Phys. Lett.*, (410), 321–323.
- [13] Neri, G., Bonavita, A., Pizzo, G., Galvagno, S., Donato, N., Caputi, L.S., (2004). A study of water influence on CO response on gold-doped iron oxide sensors. *Sensor. Actuat. B-Chem.*, (101), 90–96.
- [14] Balasubramaniana, S., Panigrahi, S., Logue, C.M., Gu, H., Marchello, M., (2009). Neural networks-integrated metal oxide-based artificial olfactory system for meat spoilage identification. *J. Food Eng.*, (91), 91–98.
- [15] Lee, D.S., Ban, S.W., Lee, M., Lee, D.D., (2005). Micro gas sensor array with neural network for recognizing combustible leakage gases. *IEEE Sensor. J.*, (5), 530–536.
- [16] Kermani, B.G., Schiffman, S.S., Nagle H.T., (2005). Performance of the Levenberg–Marquardt neural network training method in electronic nose applications. *Sensor. Actuat. B-Chem.*, (110), 13–22.
- [17] Pławiak, P., Maziarz, W., (2014). Classification of tea specimens using novel hybrid artificial intelligence methods. *Sensor. Actuat. B-Chem.*, (192) 117–125.
- [18] Ortega, A., Marco, S., Perera, A., Šundic, T., Pardo A., Samitier J., (2001). An intelligent detector based on temperature modulation of a gas sensor with a digital signal processor. *Sensor. Actuat. B-Chem.*, (78), 32–39.
- [19] Nakata, S., Okunishi, H., Nakashima, Y., (2006). Distinction of gases with a semiconductor sensor under a cyclic temperature modulation with second-harmonic heating. *Sensor. Actuat. B-Chem.*, (119) 556–561.
- [20] Ionescu, R., Llobet, E., (2002). Wavelet transform-based fast feature extraction from temperature modulated semiconductor gas sensors. *Sensor. Actuat. B-Chem.*, (81) 289–295.
- [21] Huang, X. J., Choi, Y. K., Yun, K. S., Yoon, E., (2006). Oscillating behaviour of hazardous gas on tin oxide gas sensor: Fourier and wavelet transform analysis. *Sensor. Actuat. B-Chem.*, (115) 357–364.
- [22] Szczówka, P. M., Szczurek, A., Licznerski, B.W., (2011). On reliability of neural network sensitivity analysis applied for sensor array optimization. *Sensor. Actuat. B-Chem.*, (157) 298–303.
- [23] Ngo, K. A., Lauque, P., Aguir, K., (2007). High performance of a gas identification system using sensor array and temperature modulation. *Sensor. Actuat. B-Chem.*, (124) 209–216.
- [24] Huang, J. R., Gu, C. P., Meng, F. L., Li, M. Q., Liu, J. H., (2007). Detection of volatile organic compounds by using a single temperature-modulated SnO<sub>2</sub> gas sensor and artificial neural network. *Sensors*, (16) 209–216.
- [25] Technical data about the UST GGS sensors published on <http://www.umweltsensortechnik.de> (May 2013).